J Biomol NMR (2009) 45:329–334
DOI 10.1007/s10858-009-9361-8

NMR STRUCTURE NOTE

# Solution structure of the human Tax-interacting protein-1

**Michael A. Durney · Gabriel Birrane · Clemens Anklin · Aditi Soni · John A. A. Ladias**

Received: 28 May 2009 / Accepted: 23 July 2009 / Published online: 15 August 2009


## Biological context

PDZ (PSD95/DLG/ZO-1) domains are protein–protein interaction modules composed of 90–100 amino acids. PDZ-containing proteins function in the organization of multiprotein complexes at specific cellular sites and control the spatial and temporal fidelity of intracellular signaling pathways. The PDZ fold comprises a compact six-stranded $\beta$-barrel ($\beta$1–$\beta$6) capped by two $\alpha$-helices ($\alpha$1–$\alpha$2) (Doyle et al. 1996). Target protein recognition is accomplished via a long and deep groove formed between $\beta$2 and $\alpha$2. The C terminus of target proteins inserts into this groove and augments the $\beta$-sheet structure of the domain. Certain PDZ domains interact with internal sequence motifs, whereas others bind lipids. Previous studies have established three PDZ classes based on their consensus recognition sequence. Class I prefer X-S/T-X-Φ-COOH, class II interact with X-Φ-X-Φ-COOH, and class III recognize X-D/E-X-Φ-COOH, where X is any amino acid and Φ is a hydrophobic residue. However, many PDZ domains bind promiscuously to targets from different classes, underscoring the need for a new classification scheme (Birrane et al. 2003).

In general, PDZ proteins possess multiple domains facilitating their functions as protein–protein interaction modules in a variety of cellular contexts. The human Tax-interacting protein-1 (TIP-1) is an unusual PDZ protein predicted to be comprised entirely of a single PDZ domain. TIP-1 was initially identified as an interaction partner of the human T-lymphotropic virus type 1 (HTLV-1) Tax protein, a key viral regulatory protein involved in deregulating numerous cellular signal transduction pathways (Rousset et al. 1998). TIP-1 was also independently identified as a protein that associates with glutaminase L and was termed glutaminase-interacting protein (Olalla et al. 2001). TIP-1 participates in Rho signaling through its interaction with Rhotekin (Reynaud et al. 2000). In addition, TIP-1 binds with high affinity to the C terminus of $\beta$-catenin and inhibits its transcriptional activity (Kanamori et al. 2003). TIP-1 also interacts with the C-terminal tail of the Kir 2.3 potassium channel and functions as a negative regulator of its surface expression (Alewine et al. 2006).

As a first step towards understanding the structural basis of TIP-1 interaction with cellular and viral proteins, we determined the solution structure of TIP-1 in the apo form and studied its interaction with a Kir 2.3 C-terminal peptide, using nuclear magnetic resonance (NMR) spectroscopy. We show that TIP-1 consists of a single PDZ domain flanked by unstructured N and C termini. Unique features of the TIP-1 PDZ domain include a short, two-stranded $\beta$-sheet within its $\beta$1–$\beta$2 loop, and a long $\beta$2–$\beta$3 loop that may participate in ligand binding. Extensive chemical shift perturbations are observed during titration of the protein with a Kir 2.3 peptide, indicating that TIP-1 undergoes conformational changes upon interaction with target proteins.

M. A. Durney · G. Birrane · A. Soni · J. A. A. Ladias (✉)
Molecular Medicine Laboratory and Macromolecular Crystallography Unit, Department of Medicine, Harvard Medical School, Boston, MA 02215, USA
e-mail: johnladias@gmail.com

M. A. Durney
Department of Molecular and Cellular Biology, Harvard University, Cambridge, MA, USA

C. Anklin
Bruker BioSpin Corporation, Billerica, MA, USA

## Methods and results

### Protein expression and purification

A DNA fragment encoding human TIP-1 (residues 2–124) was amplified by PCR and cloned into a modified pMAL-c2X vector (New England Biolabs). Unlabeled recombinant TIP-1 was expressed as a hexahistidine-tagged fusion to maltose-binding protein in *E. coli* C41(DE3) cells (Novagen) by growing LB cultures to an $OD_{600}$ of $\sim$0.6 followed by induction at 37°C with 1 mM IPTG for 5 hours. Isotope labeling was performed using a media-exchange method (Marley et al. 2001). For this method, cells were grown in LB to an $OD_{600}$ of $\sim$0.7, pelleted by centrifugation, washed once in M9 salts, resuspended in 25% volume M9 minimal media containing $^{15}NH_4Cl$ and $^{13}C$-glucose as the sole nitrogen and carbon sources. Minimal media cultures were incubated for 1 hour before induction at 37°C with 1 mM IPTG for 5 hours.

Cell pellets were resuspended on ice in PBS supplemented with 200 mM NaCl and EDTA-free protease inhibitor cocktail tablets (Roche Applied Sciences) and lysed on an EmulsiFlex-C3 homogenizer (Avestin). Cell debris was pelleted by centrifugation and the clear supernatant was purified in batch mode using Ni-NTA affinity resin. TIP-1 was cleaved from the fusion protein with thrombin and concentrated by ultracentrifugation. The protein was further purified by size exclusion chromatography on a Superdex 75 column (GE-Healthcare) to apparent homogeneity, as judged by SDS-PAGE.

### NMR experiments

Purified TIP-1 protein was exchanged into NMR buffer composed of 50 mM sodium phosphate pH 6.5, 50 mM NaCl, 1 mM EDTA, 1 μM $NaN_3$. All NMR experiments were performed at 298 K on Bruker 600 MHz and 700 MHz spectrometers equipped with cryoprobes. CBCA(CO)HN, HNCA, HNCACB and HNCO backbone assignments were obtained using a minimal set of triple resonance experiments recorded using a $\sim$1.0 mM $^{13}C$-/$^{15}N$-labeled sample. Side chain assignments were obtained using the HCCH-COSY, CC(CO)NH-TOCSY and HC(CO)NH-TOCSY experiments. Aromatic protons were assigned using a $^{13}C$-edited NOESY-HSQC. Amine side chains of asparagine and glutamine residues were assigned from a NOESY-HSQC experiment recorded on a $^{15}N$-labeled sample. Data were processed using NMRPipe (Delaglio et al. 1995) and assigned using NMRView (Johnson and Blevins 1994). The majority of the resonances were assigned including the flexible termini of the protein which, although unstructured (see below), have a high level of sequence conservation across species (Fig. 1a).

### Structure calculations

Input for the structure determination consisted of distance restraints from NOE spectra and torsion angle restraints derived from chemical shift data by TALOS (Cornilescu et al. 1999). The structure of TIP-1 was determined using 2548 distance restraints and 124 dihedral angle restraints. A small subset of the NOE data was assigned manually using resonances with distinctive chemical shifts allowing unambiguous assignment. The remaining peaks in the $^{13}C$- and $^{15}N$-edited NOESY spectra were picked manually and formed the basis of automated assignment and structure calculation by CYANA (Güntert et al. 1997). The coordinates were refined in explicit solvent using CNS (Brünger et al. 1998) and the RECOORD protocols (Nederveen et al. 2005) leading to an improved Ramachandran plot and packing quality (Table 1). Structures were visualized using PyMOL (www.pymol.org). Structure quality was assessed using PROCHECK-NMR (Laskowski et al. 1996). For the ensemble of structures, less than 1% of residues are in the disallowed region of the Ramachandran plot.

The structure of TIP-1 is comprised of a PDZ domain flanked by flexible termini (Fig. 1b, c). The termini of TIP-1 are unstructured in solution as evidenced by the lack of NOE data and intense resonances clustered in the center of the spectrum for these residues. The PDZ domain is very similar to previously determined structures and presents the expected topological arrangement of secondary structure elements. In addition to the canonical PDZ secondary structure elements, there are two relatively long structured loops inserted between the $\beta$-strands. The $\beta1$–$\beta2$ loop contains a two-stranded $\beta$-sheet (Fig. 1a–c) not observed in other PDZ domains. The TIP-1 $\beta2$–$\beta3$ loop is four amino acid residues longer than the corresponding loop of the Erbin PDZ, which was previously shown to contribute to ligand binding (Birrane et al. 2003) suggesting a similar role for this loop in TIP-1. Importantly, the Erbin PDZ sequence motif 1304-NPF-1306 within the $\beta2$–$\beta3$ loop that mediates interaction with Tyr -7 of the ligand (Birrane et al. 2003) is highly conserved in TIP-1 across species (Fig. 1a), suggesting that the TIP-1 residues Asn44, Pro45, and Phe46 may also participate in ligand binding. The PDZ domain of our TIP-1 solution structure and a recent X-ray structure (Zhang et al. 2008) superimpose over main chain atoms in residues 14–110 with a root mean square deviation (RMSD) of 1.90 Å, and 1.54 Å over the secondary structure elements (Fig. 1d). We omitted the termini for the calculation of the RMSD since both the N and C termini are unstructured in solution. In contrast, the C terminus of the unbound full-length crystal structure is α-helical, possibly as a result of crystal packing interactions (Zhang et al. 2008).

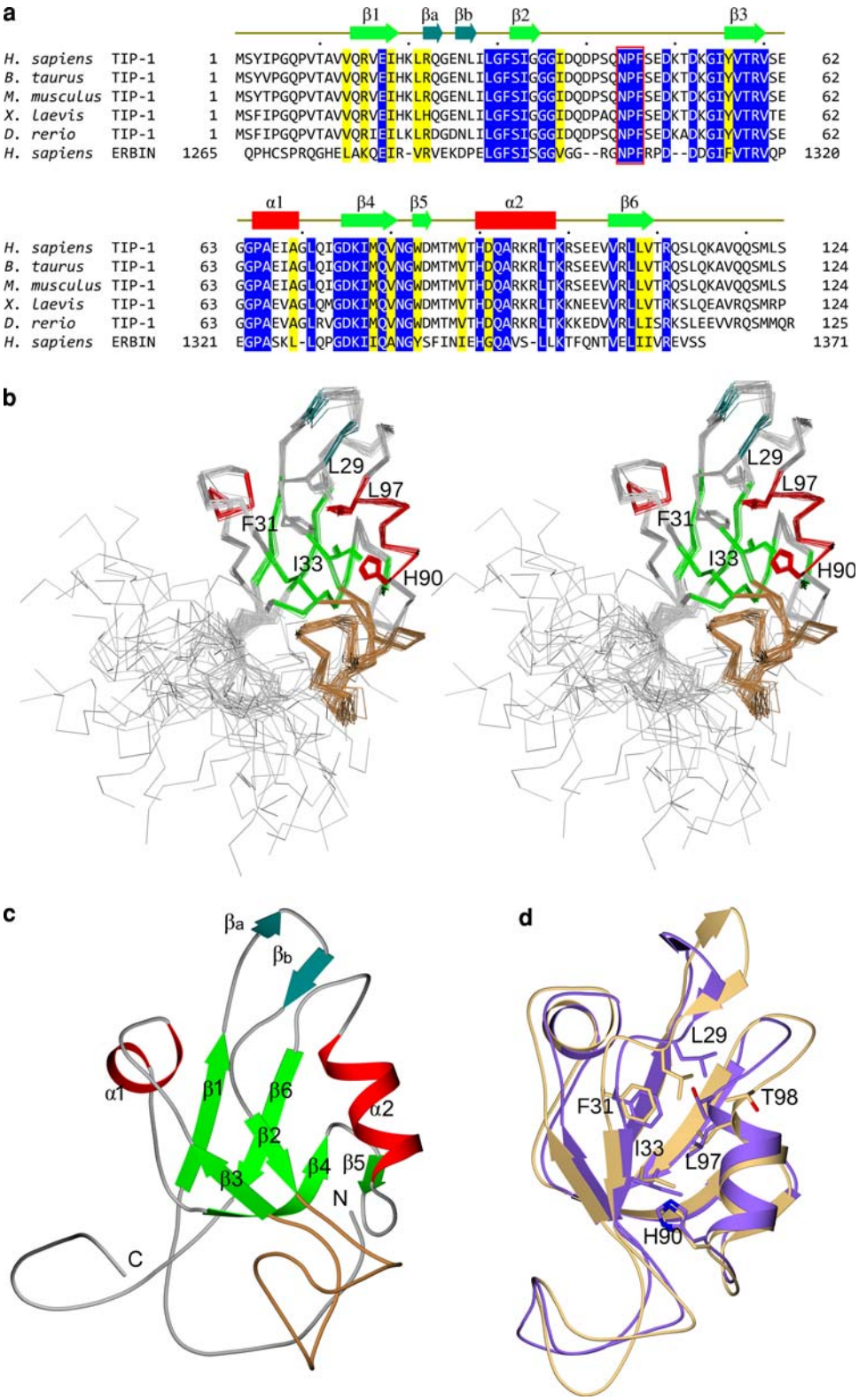


**Fig. 1** Sequence and structural analysis of the human TIP-1 protein. **a** Alignment of TIP-1 from selected species and the human Erbin PDZ. Canonical PDZ α-helices and *β*-strands are colored *red* and *green*, respectively, whereas the unique strands *β*a and *β*b are colored *cyan*. Identical residues are shown as *white* letters on *blue* background and similar residues are highlighted in *yellow*. The conserved residues NPF, which participate in ligand recognition by the Erbin PDZ, are enclosed in a *red* box. **b** Stereo view of an ensemble representing the 20 TIP-1 water-refined structures. Secondary structure elements are colored as in Fig. 1a with the extended *β*2–*β*3 loop colored *beige*. **c** Secondary structure representation of TIP-1. **d** Superposition of the solution (*beige*) and crystal (*purple*) structures of unbound TIP-1 (PDB code 3DJ1). Side chains of residues in the binding pocket are shown as *stick* models. Figure 1b–d was generated with POV-Ray (www.povray.org)

## Isothermal titration calorimetry and NMR titration experiments

To study the interaction between TIP-1 and Kir 2.3 we analyzed complex formation between TIP-1 and the synthetic peptide NISYRRESAI corresponding to the C-terminal sequence of the channel. Binding constants for the interaction of TIP-1 with the Kir 2.3 peptide were measured using a VP-ITC microcalorimeter (MicroCal). Briefly, ~0.45 mM Kir 2.3 peptide was titrated into a

**Table 1** Statistics for the final ensemble of 20 water-refined structures of TIP-1

| | |
|---|---|
| Experimental restraints | |
| Short-range NOEs ($\|i-j\| \leq 1$) | 1,234 |
| Medium-range NOEs ($1 < \|i-j\| < 5$) | 469 |
| Long-range NOEs ($\|i-j\| \geq 5$) | 845 |
| Total NOEs | 2,548 |
| Restraint violations | |
| NOE distances with violations > 0.3 Å | 0.65 ± 0.67 |
| RMSD from experimental restraints | |
| All distance restraints (Å) | 0.0217 ± 0.0011 |
| CNS energy (kcal/mol) | |
| $E_{ELEC}$ | −4593.7 ± 122.0 |
| $E_{VDW}$ | −428.71 ± 14.60 |
| RMSD from idealized covalent geometry | |
| Bond lengths (Å) | 0.0127 ± 0.0004 |
| Bond angles (°) | 1.40 ± 0.04 |
| Impropers (°) | 1.59 ± 0.08 |
| Ramachandran plot statistics | |
| Most favored regions | 80.3% |
| Additionally allowed regions | 17.0% |
| Generously allowed regions | 1.8% |
| Disallowed regions | 0.9% |
| Coordinate RMSD (residues 10–110, average to mean, Å) | |
| Ordered backbone atoms | 0.473 |
| Ordered heavy atoms | 0.888 |

~0.05 mM solution of TIP-1 protein in 50 mM sodium phosphate, pH 6.5, 50 mM NaCl, 1 mM EDTA at 25°C. Titration curves were analyzed using ORIGIN 7.0 (OriginLab). Protein and peptide concentrations were determined by quantitative amino acid analysis on an ABI 420A derivatizer/analyzer and an ABI 130A separation system (Applied Biosystems). Experiments repeated in triplicate yielded a dissociation constant of 45.1 ± 11.4 μM when fitted using a single binding site model (Fig. 2a).

To further assess the binding affinity and specificity of the TIP-1 protein for the Kir 2.3 peptide, we employed a chemical shift perturbation analysis of NMR data of $^{15}$N-labeled protein titrated with unlabeled peptide. Titration experiments were performed by adding aliquots of a ~2.0 mM Kir 2.3 peptide solution to a ~0.5 mM $^{15}$N-labeled sample of TIP-1 and recording HSQC spectra at each titration point. The HSQC spectrum of isolated TIP-1 is indicative of a properly folded protein, presenting well-dispersed resonance peaks with uniform line widths. Titration of peptide into the protein induces perturbations in a majority of peaks indicating formation of a specific complex with direct or indirect effects on residues throughout the sequence (Fig. 2b). Our conclusion, supported by the ITC data, is that a single stoichiometric complex is formed. Upon complex formation, a significant fraction of residues undergo small resonance shifts and therefore appear in fast exchange, while a subset of residues experience larger shifts and are in slow exchange (Fig. 2c). These residues are localized primarily in the binding pocket formed by the α2 helix and β2 strand and the β2–β3 loop (Fig. 2d). Specifically, slow exchange is observed for residues Ile28, Leu29, Gly30, and Phe31 in the carboxylate-binding motif and residues Gln39 and Phe46 in the β2–β3 loop, indicating a possible role for the Kir 2.3 Tyr -6 in the interaction similar to that of Tyr -7 in the Erbin–ErbB2 complex (Birrane et al. 2003). Additionally, Asn44 undergoes a relatively large perturbation that, in conjunction with Phe46, indicates a role for the NPF motif in ligand recognition (Fig. 2d).

## Discussion and conclusions

The greatest differences between the structured regions of the crystal and solution structures of the unbound form of TIP-1 are observed within the βa–βb region, the β2–β3 loop and the carboxylate-binding pocket. Furthermore, the carboxylate-binding pocket in the solution structure is deeper due to a difference in the position of the Leu 29 side chain, and narrower due to a difference in the overall position of Thr98, giving rise to a more closed carboxylate-binding pocket in the unbound solution structure. These results are in agreement with the recently described structural changes induced in TIP-1 upon binding to peptide ligands (Banerjee et al. 2008; Zhang et al. 2008). Such conformational transitions are not unprecedented since flexible binding sites may enable recognition of diverse targets, especially for "promiscuous" proteins such as TIP-1. For example, the binding cleft of the promiscuous Dishevelled PDZ domain is more flexible than canonical PDZ domains (Zhang et al. 2009). Recently, the binding pocket of the LARG PDZ domain was also shown to be flexible and to exhibit mixed-exchange NMR spectra upon titration with a peptide representing a binding partner (Liu et al. 2008). Similarly, the second PDZ domain of human tyrosine phosphatase 1E undergoes a combination of structural and dynamical changes upon binding (Dhulesia et al. 2008). Since TIP-1 is at the junction of several different signaling pathways, such plasticity may in fact be essential for its function. PDZ domains are capable of a very diverse range of conformational transitions that may be averaged to differing extents in crystal and solution conditions. Ongoing NMR studies of the structure and dynamics of TIP-1 complexes will yield insights into the exact nature of the conformational transitions associated with binding.

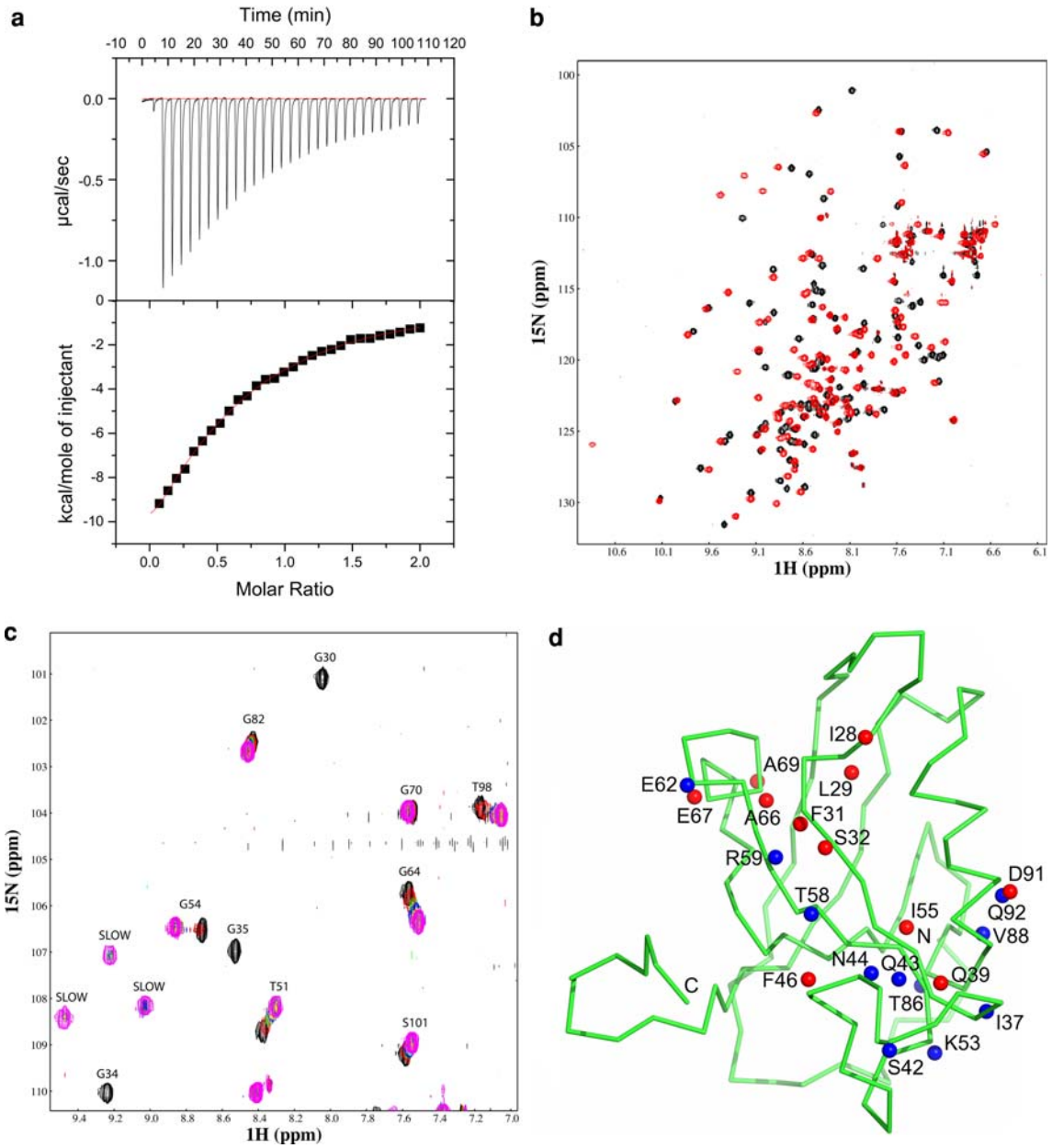


**Fig. 2** Specific complex formation between the TIP-1 protein and the Kir 2.3 peptide. **a** Isothermal titration calorimetry data obtained for the interaction of TIP-1 with the Kir 2.3 peptide as described in the text. **b** HSQC spectra of TIP-1 in the absence (*black contours*) and presence (*red contours*) of Kir 2.3 peptide. **c** Selected region of HSQC spectra highlighting chemical shift perturbations induced by increasing molar ratios of Kir 2.3 peptide to TIP-1 protein. Resonances in fast exchange are labeled with *residue numbers* and complex resonances in slow exchange are labeled "*SLOW*". **d** Structural mapping of chemical shift perturbations for the TIP-1 interaction with the Kir 2.3 C-terminal peptide. Residues in slow exchange are shown as *red* spheres and residues in fast exchange with perturbations one standard deviation above the mean are depicted as *blue* spheres. The figure was generated with PyMOL (www.pymol.org)

In conclusion, our solution structure of human TIP-1 shows that it consists of a single PDZ domain flanked by unstructured termini. The TIP-1 PDZ contains an additional two-stranded $\beta$-sheet within its $\beta1$–$\beta2$ loop, and a long $\beta2$–$\beta3$ loop that may participate in ligand binding. The extensive chemical shift perturbations observed upon interaction with the Kir 2.3 peptide indicate that TIP-1 undergoes conformational changes during binding to target proteins.

## Database accession numbers

The coordinates of the 20 refined TIP-1 structures have been deposited in the Protein Data Bank (PDB entry

2KG2) and the chemical shift data have been deposited at the BMRB (entry 16285).

**Acknowledgments** We thank Robert Griffin and Tony Bielecki for NMR access at the MIT/Harvard Center for Magnetic Resonance (funded by NIH grant EB-002026), and George Whitesides, Harvard University, for access to ITC instrumentation. This work was supported by grants GM065520, DK062162, and AG021964 from the National Institutes of Health, DAMD170210300, DAMD170310563, W81XWH0510622, and W81XWH0710178 from the US Department of Defense, a grant from the Dystonia Medical Research Foundation, and the Temple Discovery Award TLL035927 from the Alzheimer's Association to J.A.A.L.

## References

Alewine C, Olsen O, Wade JB, Welling PA (2006) TIP-1 has PDZ scaffold antagonist activity. Mol Biol Cell 17:4200–4211

Banerjee M, Huang C, Marquez J, Mohanty S (2008) Probing the structure and function of human glutaminase-interacting protein: a possible target for drug design. Biochemistry 47:9208–9219

Birrane G, Chung J, Ladias JAA (2003) Novel mode of ligand recognition by the Erbin PDZ domain. J Biol Chem 278: 1399–1402

Brünger AT, Adams PD, Clore GM, DeLano WL, Gros P, Grosse-Kuntstleve RW, Jiang JS, Kuszewski J, Nilges M, Pannu NS, Read RJ, Rice LM, Simoson T, Warren GL (1998) Crystallography & NMR system: a new software suite for macromolecular structure determination. Acta Crystallogr Sect D: Biol Crystallogr 55:905–921

Cornilescu G, Delaglio F, Bax A (1999) Protein backbone angle restraints from searching a database for chemical shift and sequence homology. J Biomol NMR 13:289–302

Delaglio F, Grzesiek S, Vuister G, Zhu G, Pfeifer J, Bax A (1995) NMRPipe: a multidimensional spectral processing system based on UNIX pipes. J Biomol NMR 6:277–293

Dhulesia A, Gsponer J, Vendruscolo M (2008) Mapping of two networks of residues that exhibit structural and dynamical changes upon binding in a PDZ domain protein. J Am Chem Soc 130:8931–8939

Doyle DA, Lee A, Lewis J, Kim E, Sheng M, MacKinnon R (1996) Crystal structures of a complexed and peptide-free membrane protein-binding domain: molecular basis of peptide recognition by PDZ. Cell 85:1067–1076

Güntert P, Mumenthaler C, Wüthrich K (1997) Torsion angle dynamics for NMR structure calculation with the new program DYANA. J Mol Biol 273:283–298

Johnson BA, Blevins RA (1994) NMRView: a computer program for the visualization and analysis of NMR data. J Biomol NMR 4:603–614

Kanamori M, Sandy P, Marzinotto S, Benetti R, Kai C, Hayashizaki Y, Schneider C, Suzuki H (2003) The PDZ protein Tax-interacting protein-1 inhibits beta-catenin transcriptional activity and growth of colorectal cancer cells. J Biol Chem 278:38758–38764

Laskowski RA, Rullmann JA, MacArthur MW, Kaptein R, Thornton JW (1996) AQUA and PROCHECK-NMR: programs for checking the quality of protein structures solved by NMR. J Biomol NMR 8:477–486

Liu J, Zhang J, Yang Y, Huang H, Shen W, Hu Q, Wang X, Wu J, Shi Y (2008) Conformational change upon ligand binding and dynamics of the PDZ domain from leukemia-associated Rho guanine nucleotide exchange factor. Protein Sci 17:1003–1014

Marley J, Lu M, Bracken C (2001) A method for efficient isotopic labeling of recombinant proteins. J Biomol NMR 20:71–75

Nederveen A, Doreleijers JF, Vranken W, Miller Z, Spronk CA, Nabuurs SB, Güntert P, Livny M, Markley JL, Nilges M, Ulrich EL, Kaptein R, Bonvin AM (2005) RECOORD: a recalculated coordinate database of 500+ proteins from the PDB using restraints from the BioMagResBank. Proteins 59:662–672

Olalla L, Aledo JC, Bannenberg G, Márquez J (2001) The C-terminus of human glutaminase L mediates association with PDZ domain-containing proteins. FEBS Lett 488:116–122

Reynaud C, Fabre S, Jalinot P (2000) The PDZ protein TIP-1 interacts with the Rho effector rhotekin and is involved in Rho signaling to the serum response element. J Biol Chem 275:33962–33968

Rousset R, Fabre S, Desbois C, Bantignies F, Jalinot P (1998) The C-terminus of the HTLV-1 Tax oncoprotein mediates interaction with the PDZ domain of cellular proteins. Oncogene 16:643–654

Zhang J, Yan X, Shi C, Yang X, Guo Y, Tian C, Long J, Shen Y (2008) Structural basis of $\beta$-catenin recognition by Tax-interacting protein-1. J Mol Biol 384:255–263

Zhang Y, Appleton BA, Weismann C, Lau T, Costa M, Hannoush RN, Sidhu SS (2009) Inhibition of Wnt signaling by dishevelled PDZ peptides. Nat Chem Biol 5:217–219